Organometallics **2005,** *24,* 5431−5439

Reversible Isomerization of a Diphosphine Ligand about a Triosmium Cluster: Synthesis, Kinetics, and X-ray Structures for the Bridging and Chelating Isomers of $Os_3(CO)_{10}[(Z)\text{-}Ph_2PCH{=}CHPPh_2]$

William H. Watson*

Department of Chemistry, Texas Christian University, Fort Worth, Texas 76129

Guanmin Wu and Michael G. Richmond*

Department of Chemistry, University of North Texas, Denton, Texas 76203

Received June 29, 2005

Substitution of the MeCN ligands in the activated cluster $Os_3(CO)_{10}(MeCN)_2$ (**1**) by the unsaturated diphosphine ligand (Z)-$Ph_2PCH{=}CHPPh_2$ proceeds rapidly at room temperature to furnish the ligand-bridged cluster 1,2-$Os_3(CO)_{10}[(Z)\text{-}Ph_2PCH{=}CHPPh_2]$ (**2b**). Heating **2b** leads to the formation of the thermodynamically more stable chelating isomer 1,1-$Os_3(CO)_{10}[(Z)\text{-}Ph_2PCH{=}CHPPh_2]$ (**2c**). The molecular structure of each isomer of **2** has been crystallographically determined, and the ^{31}P NMR data have been recorded. The kinetics for the ligand isomerization have been investigated by UV−vis and ^{31}P NMR spectroscopy in toluene solution over the temperature range of 358−383 K. The reversible nature of the diphosphine isomerization is confirmed by ^{31}P NMR measurements, and reported within are the forward (k_1) and reverse (k_{-1}) first-order rate constants for the bridge-to-chelate rearrangement. On the basis of the activation parameters and lack of CO inhibition on the reaction rate, a nondissociative, intramolecular mechanism involving the migration of one P group from an adjacent osmium center to the other P-substituted osmium center via a μ_2-bridged phosphine species is presented.

Introduction

The reaction of bidentate phosphines with the activated triosmium clusters $Os_3(CO)_{12-n}(MeCN)_n$ (n = 1, 2) and $Os_3(CO)_{10}L_2$ (L_2 = 1,5-cod, 1,3-butadiene) has been investigated over the years with respect to the bonding mode adopted by the bidentate P ligand upon coordination.[1−3] Simple coordination of diphosphine ligands at these activated clusters typically proceeds to furnish a bridged or chelated cluster $Os_3(CO)_{10}(P{-}P)$, where the P−P ligand is bound to adjacent osmium centers or attached to a single osmium atom:

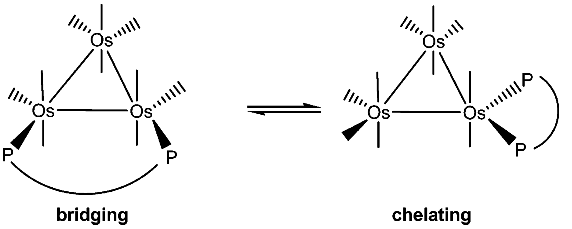

While several unequivocal examples exist for the isomerization of a diphosphine ligand at other polynuclear clusters,[4,5] no such studies have been reported for the family of $Os_3(CO)_{10}(P{-}P)$ clusters. The resulting $Os_3(CO)_{10}(P{-}P)$ clusters have been shown to exhibit some interesting chemistry, due to phosphine-assisted stabilization of cluster unsaturation. For example, the triosmium cluster $HOs_3(CO)_8[PhP(C_6H_4)CH_2PPh_2]$, which may be isolated from the thermolysis of $Os_3(CO)_{10}(dppm)$,[6] is electronically unsaturated by virtue of its 46-valence-electron count and readily undergoes a wide variety of ligand addition reactions under mild conditions.[7] The inherent unsaturation associated with the valence-electron count notwithstanding, $HOs_3(CO)_8[PhP(C_6H_4)CH_2PPh_2]$ and related clusters also possess a "masked site" of unsaturation whose origin derives from a reversible reductive coupling of the bridging hydride ligand with the μ,η^1-carbon atom of the ortho-metalated aryl ring. Such a rapid and reversible activa-

---

* To whom correspondence should be addressed. Tel: 817-257-7195 (W.H.W.); 940-565-3548 (M.G.R.). E-mail: w.watson@tcu.edu (W.H.W.); cobalt@unt.edu (M.G.R.).

(1) (a) Deeming, A. J.; Donovan-Mtunzi, S.; Kabir, S. E. *J. Organomet. Chem.* **1984**, *276*, C65; **1987**, *333*, 253. (b) Deeming, A. J.; Kabir, S. E. *J. Organomet. Chem.* **1988**, *340*, 359. (c) Deeming, A. J.; Donovan-Mtunzi, S.; Hardcastle, K. I.; Kabir, S. E.; Henrick, K.; McPartlin, M. *J. Chem. Soc., Dalton Trans.* **1988**, 579. (d) Deeming, A. J.; Stchedroff, M. *J. Chem. Soc., Dalton Trans.* **1998**, 3819.

(2) Cartwright, S.; Clucas, J. A.; Dawson, R. H.; Foster, D. F.; Harding, M. M.; Smith, A. K. *J. Organomet. Chem.* **1986**, *302*, 403.

(3) Poë, A. J.; Sekhar, V. C. *J. Am. Chem. Soc.* **1984**, *106*, 5034.

(4) (a) Shapley, J. R.; Richter, S. I.; Churchill, M. R.; Lashewycz, R. A. *J. Am. Chem. Soc.* **1977**, *99*, 7384. (b) Churchill, M. R.; Lashewycz, R. A. *Inorg. Chem.* **1978**, *17*, 1950. (c) Churchill, M. R.; Lashewycz, R. A.; Shapley, J. R.; Richter, S. I. *Inorg. Chem.* **1980**, *19*, 1277. (d) Puga, J.; Arce, A.; Braga, D.; Centritto, N.; Grepioni, F.; Castillo, R.; Ascanio, J. *Inorg. Chem.* **1987**, *26*, 867.

(5) (a) Yang, K.; Smith, J. M.; Bott, S. G.; Richmond, M. G. *Organometallics* **1993**, *12*, 4779. (b) Bott, S. G.; Yang, K.; Richmond, M. G. *J. Organomet. Chem.* **2005**, *690*, 3067.

(6) Clucas, J. A.; Foster, D. F.; Harding, M. M.; Smith, A. K. *J. Chem. Soc., Chem. Commun.* **1984**, 949.

10.1021/om0505413 CCC: $30.25

tion of the ancillary diphosphine ligand has the ability to furnish a transient cluster intermediate capable, in theory, of multisite substrate activation and cluster-promoted catalysis.[8]

In comparison to the extensive number of known $Os_3(CO)_{10}(P-P)$ clusters possessing a diphosphine ligand with a saturated carbon backbone, fewer paradigms of diphosphine derivatives that possess an unsaturated carbon backbone are known,[9,10] prompting our exploration of the reaction of $Os_3(CO)_{10}(MeCN)_2$ with (*Z*)-$Ph_2PCH{=}CHPPh_2$. This particular ligand, which is the unsaturated analogue of 1,2-bis(diphenylphosphino)ethane (dppe or diphos), has not been examined, to our knowledge, for its reactivity with simple triosmium clusters.[11] Herein we report our data on the synthesis of 1,2-$Os_3(CO)_{10}$[(*Z*)-$Ph_2PCH{=}CHPPh_2$] and, more importantly, its interconversion to the corresponding chelating isomer 1,2-$Os_3(CO)_{10}$[(*Z*)-$Ph_2PCH{=}CHPPh_2$]. Both cluster products have been structurally characterized, and the kinetics for the ligand isomerization have been investigated, providing strong evidence for a facile, nondissociative intramolecular rearrangement of the ancillary phosphine about the Os_3 frame.

Experimental Section

General Considerations. The activated cluster $Os_3(CO)_{10}(MeCN)_2$ was synthesized from $Os_3(CO)_{12}$ according to the published procedure,[12] while the parent cluster $Os_3(CO)_{12}$ was prepared from OsO_4 and CO using a 500 mL Series 4571 Parr autoclave.[13] The diphosphine ligand (*Z*)-$Ph_2PCH{=}CHPPh_2$ and $Me_3NO{\cdot}2H_2O$ were both purchased from Aldrich Chemical Co., with the former chemical used as received and the latter dried by azeotropic distillation from benzene. The ^{13}CO (>99%) used in the synthesis of the ^{13}CO-enriched $Os_3(CO)_{12}$ was purchased from Isotec Inc. and used as received. The reaction and NMR solvents were purified by distillation under argon from an appropriate drying agent. All distilled solvents were handled under argon and stored in Schlenk vessels equipped with Teflon stopcocks.[14] The photochemical experiments were performed at room temperature with either GE blacklight bulbs, having a maximum output of 366 ± 20 nm, or a 200 W Oriel Hg(Xe) arc lamp. The combustion analyses on clusters **2b**,**c** were performed by Atlantic Microlab, Norcross, GA.

The reported infrared data were recorded on a Nicolet 20 SXB FT-IR spectrometer in 0.1 mm amalgamated NaCl cells, using PC control and OMNIC software, while the ^1H and ^{13}C NMR spectra were recorded at 200 and 50 MHz, respectively, on a Varian Gemini-200 spectrometer. The ^{31}P NMR spectra were recorded at 121 MHz on a Varian 300-VXR spectrometer. All ^{13}C and ^{31}P NMR spectra were collected in the proton-decoupled mode. The reported ^{31}P chemical shift data were referenced to external H_3PO_4, whose chemical shift was set at δ 0.

Synthesis of 1,2-$Os_3(CO)_{10}$[(*Z*)-$Ph_2PCH{=}CHPPh_2$] from $Os_3(CO)_{10}(MeCN)_2$. To a Schlenk tube under argon containing 25 mL of CH_2Cl_2 and $Os_3(CO)_{10}(MeCN)_2$, the latter of which was prepared in situ from 0.50 g (0.55 mmol) of $Os_3(CO)_{12}$ and 91 mg (1.2 mmol) of Me_3NO, was added 0.22 g (0.56 mmol) of (*Z*)-$Ph_2PCH{=}CHPPh_2$ in 15 mL of CH_2Cl_2 via syringe. The reaction mixture was stirred overnight at room temperature, after which the solvent was removed under vacuum and purification effected by column chromatography over silia gel using CH_2Cl_2/hexanes (1:9) as the eluent. The major product that was isolated corresponded to 1,2-$Os_3(CO)_{10}$[(*Z*)-$Ph_2PCH{=}CHPPh_2$] along with a small amount of yellow $Os_3(CO)_{11}[\eta^1$-(*Z*)-$Ph_2PCH{=}CHPPh_2$], whose identity was ascertained spectroscopically and confirmed by a sample of the same that was isolated from the independent reaction of $Os_3(CO)_{11}(MeCN)$ with (*Z*)-$Ph_2PCH{=}CHPPh_2$. Recrystallization of 1,2-$Os_3(CO)_{10}$[(*Z*)-$Ph_2PCH{=}CHPPh_2$] from CH_2Cl_2/hexane gave cluster **2b** as an analytically pure yellow-orange solid. Yield: 0.47 g (67%). IR (CH_2Cl_2): ν(CO) 2088 (s), 2025 (s), 2013 (vs), 2001 (vs), 1971 (s), 1949 (b, sh) cm^{-1}. ^1H NMR ($CDCl_3$): δ 6.29 (2H, m, vinyl), 6.80−7.45 (20H, m, aryl). ^{13}C NMR (toluene-d_8; 243 K): δ 173.92 (s, 2C, equatorial), 178.91 (s, 2C, equatorial), 184.96 (s, 2C, axial), 191.49 (s, 4C, axial). ^{31}P NMR ($CDCl_3$): δ −6.45. Anal. Calcd (found) for $C_{36}H_{22}O_{10}Os_3P_2$: C, 34.64 (34.95); H, 1.76 (1.78). Yield of $Os_3(CO)_{11}[\eta^1$-(*Z*)-$Ph_2PCH{=}CHPPh_2$]: 25 mg (3.6%). IR (CH_2Cl_2): ν(CO) 2107 (m), 2053 (s), 2032 (s), 2016 (vs), 2001 (s, sh), 1989 (m), 1974 (m) cm^{-1}. ^1H NMR ($CDCl_3$): δ 6.98−7.60 (22H, m, vinyl and aryl). ^{31}P NMR ($CDCl_3$): δ −16.37 (1P, d, J_{P-P} = 21 Hz), −30.65 (1P, d, J_{P-P} = 21 Hz).

Synthesis of 1,1-$Os_3(CO)_{10}$[(*Z*)-$Ph_2PCH{=}CHPPh_2$] from 1,2-$Os_3(CO)_{10}$[(*Z*)-$Ph_2PCH{=}CHPPh_2$]. To a Carius tube under argon was added 0.20 g (0.16 mmol) of 1,2-$Os_3(CO)_{10}$[(*Z*)-$Ph_2PCH{=}CHPPh_2$] and 15 mL of toluene, after which CO was bubbled through the solution for several minutes prior to sealing the tube. The reaction mixture was heated to ca. 85 °C for 22 h, and then the solution was cooled to room temperature and the solvent removed. The residue was purified by chromatography over silica gel using CH_2Cl_2/hexanes (4:6) as the eluent to afford a yellow-orange solid that actually consisted of a 1:7 mixture of 1,2- and 1,1-$Os_3(CO)_{10}$[(*Z*)-$Ph_2PCH{=}CHPPh_2$ (vide infra) by ^{31}P NMR spectroscopy. The chelating isomer was obtained free from the bridging isomer by careful recrystallization from a 1:1 mixture of CH_2Cl_2 and hexane. Yield: 80 mg (40%). IR (CH_2Cl_2): ν(CO) 2092 (m), 2042 (vs), 2006 (vs, b), 1973 (m), 1957 (m), 1926 (w, b) cm^{-1}. ^1H NMR ($CDCl_3$): δ 7.30−7.80 (22H, m, vinyl and aryl). ^{13}C NMR (toluene-d_8; 243 K): δ 171.24 (s, 2C, equatorial), 178.59 (s, 2C, equatorial), 185.34 (s, 4C, axial), 196.39 (t, 2C, axial, J_{P-C} = 9 Hz). ^{31}P NMR ($CDCl_3$): δ 37.39. Anal. Calcd (found) for $C_{36}H_{22}O_{10}Os_3P_2$: C, 34.64 (34.71); H, 1.76 (1.68).

X-ray Structural Determinations. Single crystals of clusters **2b** were grown from a CH_2Cl_2 solution containing the pure bridging isomer that had been layered with hexane, while single crystals of cluster **2c** suitable for diffraction analysis were grown from an equilibrated solution containing both isomers (ca. 85:15 mixture of **2c** and **2b**) using CH_2Cl_2 and hexane. X-ray data were collected on a Bruker SMART 1000 CCD-based diffractometer at 297(2) and 213(2) K for samples **2b**,**c**, respectively. The frames were integrated with the available SAINT software package using a narrow-frame

---

(7) (a) Deeming, A. J.; Hardcastle, K. I.; Kabir, S. E. *J. Chem. Soc., Dalton Trans.* **1988**, 827. (b) Colbran, S. B.; Irele, P. T.; Johnson, B. F. G.; Kaye, P. T.; Lewis, J.; Raithby, P. R. *J. Chem. Soc., Dalton Trans.* **1989**, 2033. (c) Brown, M. P.; Dolby, P. A.; Harding, M. M.; Mathews, A. J.; Smith, A. K. *J. Chem. Soc., Dalton Trans.* **1993**, 1671. (d) Abedin, S. M. T.; Azam, K. A.; Hursthouse, M. B.; Kabir, S. E.; Malik, K. M. A.; Mottalib, M. A.; Rosenberg, E. *J. Cluster Sci.* **2001**, *12*, 5. (e) Azam, K. A.; Hursthouse, M. B.; Islam, M. R.; Kabir, S. E.; Abdul Malik, K. M.; Miah, R.; Sudbrake, C.; Vahrenkamp, H. *J. Chem. Soc., Dalton Trans.* **1998**, 1097.

(8) (a) Lavigne, G. In *The Chemistry of Metal Cluster Complexes*; Shriver, D. F., Kaesz, H. D., Adams, R. D., Eds.; VCH: New York, 1990; Chapter 5. (b) Lavigne, G.; de Bonneval, B. In *Catalysis by Di- and Polynuclear Metal Cluster Complexes*; Adams, R. D., Cotton, F. A., Eds.; Wiley-VCH: New York, 1998; Chapter 2.

(9) (a) Clucas, J. A.; Dawson, R. H.; Dolby, P. A.; Harding, M. M.; Pearson, K.; Smith, A. K. *J. Organomet. Chem.* **1986**, *311*, 153. (b) Ang, H. G.; Ang, S. G.; Wang, X. *J. Chem. Soc., Dalton Trans.* **2000**, 3429.

(10) For a related reaction starting from a triosmium nitrate complex, see: Hui, B. K.-M.; Wong, W.-T. *J. Chem. Soc., Dalton Trans.* **1998**, 447.

(11) For the reaction between $H_4Os_4(CO)_{12}$ and (*Z*)-$Ph_2PCH{=}CHPPh_2$, see: Choi, Y.-Y.; Wong, W.-T. *J. Organomet. Chem.* **1997**, *542*, 121.

(12) Nicholls, J. N.; Vargas, M. D. *Inorg. Synth.* **1989**, *26*, 289.

(13) Drake, S. R.; Loveday, P. A. *Inorg. Synth.* **1990**, *28*, 230.

(14) Shriver, D. F. *The Manipulation of Air-Sensitive Compounds*; McGraw-Hill: New York, 1969.

algorithm,[15] and each structure was solved and refined using the SHELXTL program package.[16] The Flack parameter for structure **2b** was found to be 0.006(7), confirming the choice of absolute configuration. The molecular structure was checked by using PLATON,[17] and all non-hydrogen atoms were refined anisotropically, with the hydrogen atoms assigned calculated positions and allowed to ride on the attached heavy atom. The refinement for **2b** converged at $R = 0.0274$ and $R_w = 0.0548$ for 8700 independent reflections with $I > 2\sigma(I)$ and for **2c** at $R = 0.0448$ and $R_w = 0.0585$ for 8180 independent reflections with $I > 2\sigma(I)$.

Kinetic Studies. The UV−vis studies were carried out in toluene solution at a cluster concentration of ca. 10^{-4} M using 1.0 cm quartz UV−visible cells that were equipped with a high-vacuum Teflon stopcock to facilitate handling on the vacuum line and glovebox transfers. Stock solutions of **2b** in toluene when not in use were stored in the dark and under argon. All samples of **2b** for UV−vis kinetic experiments were saturated with CO prior to heating to suppress the formation of the hydride-bridged cluster $HOs_3(CO)_9[\mu$-(*Z*)-$PhP(C_6H_4)CH{=}CHPPh_2]$ (vide infra). The Hewlett-Packard 8452A diode array spectrometer employed in our studies was configured with a variable-temperature cell holder and was connected to a VWR constant-temperature circulator, which regulated the reaction temperature to within ±0.5 K. The ^{31}P NMR kinetic and equilibration studies were conducted in 5 mm NMR tubes that possessed a J-Young valve for the easy admission of CO gas. All NMR studies employed toluene-d_8 as a solvent with a cluster concentration of ca. 10^{-2} M. The NMR samples were heated in the same VWR temperature bath and quenched in an external ice bath immediately before NMR analysis.

The UV−vis kinetics were monitored by following the increase of the 368 nm absorbance band as a function of time for a minimum of 6 half-lives. The rate constants for the approach to equilibrium (k_e) were determined by nonlinear regression analysis using the single-exponential function[18]

$$A(t) = A_\infty + \Delta A[e^{(-k_e t)}]$$

To accurately determine the rates to equilibrium by ^{31}P NMR spectroscopy for the bridge-to-chelate isomerization starting from **2b**, we first measured the ^{31}P spin−lattice relaxation times (T_1) for the three participant clusters using the standard inversion−recovery pulse sequence.[19] The T_1 values found for the clusters **2b** (4.8 s), **2c** (1.8 s), and $HOs_3(CO)_9[\mu$-(*Z*)-$PhP(C_6H_4)CH{=}CHPPh_2]$ (an average of 2.2 s for the two different ^{31}P groups)[20] allowed us to determine an appropriate acquisition delay for the accurate collection of our kinetic and thermodynamic data free from saturation effects. Use of a 41.5° flip angle and an acquisition delay of 20 s ensured complete relaxation (>99.6%) of all ^{31}P nuclei in solution. The integrated intensities of the ^{31}P signals for clusters **2b**,**c** exhibited clean exponential decays and growths, respectively, and afforded values for k_e that were found to be in excellent agreement with those data obtained from the UV−vis experiments. The K_{eq} values reported here for the bridge $\rightleftarrows$ chelate equilibrium were determined after the isomerization reactions had reached 10 half-lives. The quoted activation parameters were calculated from plots of $\ln(k/T)$ versus T^{-1},[21] with the error limits representing deviation of the data points about the least-squares line of the Eyring plot.

Results and Discussion

I. Synthesis and Spectroscopic Data for the Isomeric Clusters $Os_3(CO)_{10}[(Z)\text{-}Ph_2PCH{=}CHPPh_2]$. The reaction between $Os_3(CO)_{10}(MeCN)_2$ (**1**) and the unsaturated diphosphine ligand (*Z*)-$Ph_2PCH{=}CHPPh_2$ proceeds rapidly and without complications at room temperature to give the ligand-bridged cluster 1,2-$Os_3(CO)_{10}[(Z)\text{-}Ph_2PCH{=}CHPPh_2]$ (**2b**) as the predominant product, along with minor amounts of $Os_3(CO)_{11}[\eta^1\text{-}(Z)\text{-}Ph_2PCH{=}CHPPh_2]$, whose origin undoubtedly comes from the mono(acetonitrile) derivative $Os_3(CO)_{11}(MeCN)$, which accompanies the preparation of **1**.[22] **2b** was purified by chromatography over silica gel and characterized in solution by IR and NMR spectroscopy. Particularly diagnostic in the characterization of **2b** was the high-field ^{31}P resonance at δ −6.45, which supports the bridging of adjacent osmium centers by the ancillary diphosphine ligand,[4c,23] with the ^1H NMR spectrum revealing the two vinyl hydrogens of the ethylene bridge at δ 6.29 as part of an AA′XX′ multiplet due to coupling with the two phosphorus centers.[24] The limiting ^{13}C NMR spectrum of a ^{13}CO-enriched sample of **2b** recorded at 243 K exhibits four singlet resonances in a 1:1:1:2 integral ratio consistent with a diphosphine-bridged cluster having idealized C_{2v} symmetry. The CO assignments for **2b** are

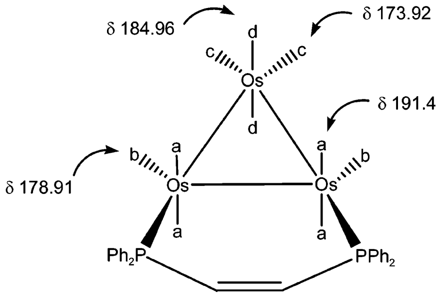

cluster **2b**

Our initial evidence for the transformation of **2b** into the chelating isomer **2c** came from a routine thermolysis study. Heating a sample of **2b** in benzene-d_6 in a sealed NMR tube at 75 °C overnight showed a diminution in the intensity of the vinyl protons of **2b** and a new ^{31}P resonance at δ 37.39, whose large nuclear deshielding is consistent with the formation of a chelating diphosphine ligand.[23] Continued heating of this same mixture for over 1 week led to the slow growth of **2c** at the expense of **2b** and establishment of an equilibrium that

---

[15] Saint Version 6.02; Bruker Analytical X-ray Systems, Inc., Madison, WI, 1997−1999.

[16] SHELXTL Version 5.1; Bruker Analytical X-ray Systems, Inc., Madison, WI, 1998.

[17] Spek, A. L. PLATON-A Multipurpose Crystallographic Tool; Utrecht University, Utrecht, The Netherlands, 2001.

[18] All rate calculations were performed with the aid of the commercially available programs Origin6.0 and KaleidaGraph. Here the initial (A_0) and final (A_∞) absorbances and the rate constant to equilibrium (k_e) were floated to give the quoted least-squares value for the first-order rate constant k_e.

[19] Sanders, J. K. M.; Hunter, B. K. *Modern NMR Spectroscopy*; Oxford University Press: New York, 1993.

[20] Our T_1 values found for the ^{31}P nuclei are in close agreement with the values determined for other phosphine-substituted inorganic/organometallic compounds. See: (a) Plourde, F.; Gilbert, K.; Gagnon, J.; Harvey, P. D. *Organometallics* **2003**, *22*, 2862. (b) Socol, S. M.; Lacelle, S.; Verkade, J. G. *Inorg. Chem.* **1987**, *26*, 3221.

[21] Carpenter, B. K. *Determination of Organic Reaction Mechanisms*; Wiley-Interscience: New York, 1984.

[22] For a study on the substitution kinetics involving MeCN replacement by group 15 ligands in this genre of cluster, see: Dahlinger, K.; Poë, A. J.; Sayal, P. K.; Sekhar, V. C. *J. Chem. Soc., Dalton Trans.* **1986**, 2145.

[23] (a) Garrou, P. E. *Chem. Rev.* **1981**, *81*, 229. (b) Richmond, M. G.; Kochi, J. K. *Inorg. Chem.* **1987**, *6*, 254.

[24] (a) Garbisch, E. W., Jr. *J. Chem. Educ.* **1968**, *45*, 480. (b) Akitt, J. W.; Mann, B. E. *NMR and Chemistry*, 4th ed.; Stanley Thornes: Cheltenham, U.K., 2000.

Scheme 1

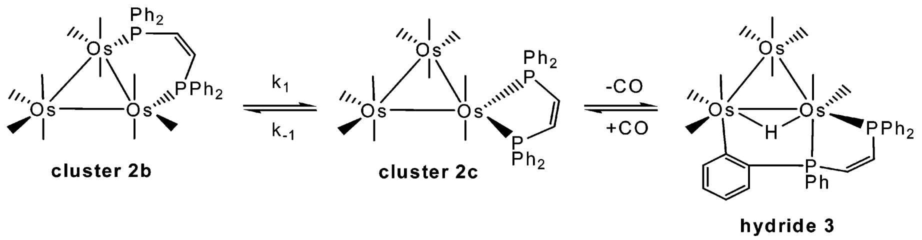

favored the chelating isomer **2c**.[25] Interestingly, TLC examination of parallel thermolysis reactions conducted in Schlenk vessels starting with **2b** showed only a single spot for the equilibrium involving **2b** and **2c**. Had this assay been the sole method of analysis, we would have missed the isomerization reaction. A trace amount of a third cluster (<1%) was also detected spectroscopically under these conditions and assigned to that of $HOs_3(CO)_9[\mu\text{-}(Z)\text{-}PhP(C_6H_4)CH{=}CHPPh_2]$, on the basis of a high-field triplet at δ −17.00 ($^2J_{P-H}$ = 13 Hz) in the ^{1}H spectrum and two nonequivalent ^{31}P resonances at δ 43.31 and 54.13.[26] The ortho metalation of the ancillary $(Z)\text{-}Ph_2PCH{=}CHPPh_2$ ligand in **2c** is a phenomenon that has been seen in related triosmium clusters containing the diphosphine ligands dppm,[6] dppe, and dppp.[7a] Thermolysis of **2b** in the presence of 1 atm of CO greatly suppressed the amount of hydride cluster formed without adversely affecting the formation of **2c**. The origin of $HOs_3(CO)_9[\mu\text{-}(Z)\text{-}PhP(C_6H_4)CH{=}CHPPh_2]$ was unequivocally demonstrated through the irradiation of samples of pure **2c** (vide infra) using near-UV light. Here the same NMR resonances (^{1}H and ^{31}P) for the hydride cluster were reproduced. The possibility of **2b** serving as the source of the hydride cluster was studied by UV−vis spectroscopy. Irradiation of **2b** with 366 nm light led to a slow bleaching of the absorption bands for **2b** with no evidence for any new species. Taken collectively, these observations strongly support the involvement of the two equilibria depicted in Scheme 1.[27]

II. X-ray Diffraction Structures for $Os_3(CO)_{10}[(Z)\text{-}Ph_2PCH{=}CHPPh_2]$. The solid-state structures of the isomeric clusters were determined by X-ray crystallography. Single crystals of cluster **2b** could be grown directly without any problems, but crystals of **2c** required more care in order to avoid the cocrystallization of both isomers of cluster **2**, which led to poor-quality X-ray crystals. Slow diffusion of hexane into a CH_2Cl_2 solution containing an equilibrium mixture of **2b** and **2c** reliably furnished small quantities of X-ray-quality crystals of **2c**. Single crystals of each cluster were found to exist as discrete molecules in the unit cell with no unusually short inter- or intramolecular contacts. Tables 1 and 2 give the pertinent X-ray processing parameters and selected bond distances and angles, respectively.

Table 1. X-ray Crystallographic Data and Processing Parameters for the Isomeric Triosmium Clusters 2b and 2c

	2b	2c
CCDC entry no.	274229	274230
space group	monoclinic, $P2_1$	monoclinic, $P2_1/n$
a, Å	12.715(3)	10.444(1)
b, Å	10.606(2)	24.115(3)
c, Å	15.128(3)	14.370(2)
β, deg	99.982(4)	100.940(2)
V, Å^3	2009.2(8)	3553.6(9)
mol formula	$C_{36}H_{22}O_{10}Os_3P_2\cdot CH_2Cl_2$	$C_{36}H_{22}O_{10}Os_3P_2$
fw	1332.00	1247.08
formula units per cell (Z)	2	4
D_{calcd}, Mg/m^3	2.202	2.331
λ(Mo Kα), Å	0.71073	0.71073
abs coeff, mm^{-1}	9.729	10.848
abs cor	empirical	empirical
max/min transmissn	0.8112/0.2635	0.8804/0.2609
total no. of rflns	16 711	29 748
no. of indep rflns	8700	8180
no. of data/restraints/params	8700/0/488	8180/0/461
R	0.0274	0.0448
R_w	0.0548	0.0585
GOF on F^2	0.945	0.921
weights	$[0.04F^2 + (\sigma F)^2]^{-1}$	$[0.04F^2 + (\sigma F)^2]^{-1}$

The Os−Os bond distances in **2b** range from 2.8642(6) Å (Os(1)−Os(2)) to 2.8774(6) Å (Os(2)−Os(3)) and display a mean distance of 2.8717 Å. The Os−Os distances are normal relative to those in other simple polynuclear osmium clusters and indicate that the triosmium frame itself does not experience any significantly adverse perturbation due to the coordination of $(Z)\text{-}Ph_2PCH{=}CHPPh_2$.[28] The 10 terminal carbonyl groups may be considered as linear with standard distances. The observed distortion or twisting of the axial CO groups in **2b** from idealized D_{3h} to D_3 symmetry is a feature common to many structurally characterized

---

[25] The rate-limiting ^{13}C NMR spectrum of a ^{13}CO-enriched sample of cluster **2c** obtained from an equilibrated sample of **2b** revealed four carbonyl resonances in a 1:1:2:1 integral ratio, of which the downfield triplet (J_{P-C} = 9 Hz) is readily ascribed to the two axial CO groups at the phosphine-substituted osmium center. The remaining chemical shifts are easily assigned by making use of the fact that the pairwise equivalent equatorial carbonyl groups appear to high field of the axial CO groups.

[26] The depicted stereochemistry for coordination of the ortho-metalated phenyl ring and the diphosphine ligand in $HOs_3(CO)_9[\mu\text{-}(Z)\text{-}PhP(C_6H_4)CH{=}CHPPh_2]$ is strengthened by a recent X-ray structure of the related hydride-bridged cluster $HOs_3(CO)_9[\mu\text{-}PhP(C_6H_4)C{=}CC(O)C({=}CHFc)C(O)PPh_2]$: Unpublished results.

[27] Additional evidence corroborating the proposed sequence depicted in Scheme 1 comes from the ligand isomerization and hydride formation in the diphosphine-substituted cluster 1,2-$Os_3(CO)_{10}$(bpcd). The isomerization of the bpcd ligand takes place under milder conditions than that of **2b** ⇄ **2c** without the formation of the corresponding hydride cluster $HOs_3(CO)_9[\mu\text{-}PhP(C_6H_4)C{=}CC(O)CH_2C(O)PPh_2]$, whose origin derives from 1,1-$Os_3(CO)_{10}$(bpcd). Detailed kinetic studies on $Os_3(CO)_{10}$(bpcd) reveal that the rates of bpcd isomerization are unaffected by added CO and phosphine trapping ligands (unpublished results). The effects of phosphine trapping ligands on the isomerization **2b** ⇄ **2c** could not be investigated, due to the competitive loss of CO in **2c** and formation of $HOs_3(CO)_9[\mu\text{-}(Z)\text{-}PhP(C_6H_4)CH{=}CHPPh_2]$.

[28] (a) Churchill, M. R.; DeBoer, B. G. *Inorg. Chem.* **1977**, *16*, 878. (b) Green, M.; Orpen, A. G.; Schaverien, C. J. *J. Chem. Soc., Dalton Trans.* **1989**, 1333. (c) Bruce, M. I.; Pain, G. N.; Hughes, C. A.; Patrick, J. M.; Skelton, B. W.; White, A. H. *J. Organomet. Chem.* **1986**, *307*, 343. (d) Adams, R. D.; Tanner, J. T. *Organometallics* **1989**, *8*, 563. (e) Constable, E. C.; Johnson, B. F. G.; Khan, F. K.; Lewis, J.; Raithby, P. R.; Mikulcik, P. *J. Organomet. Chem.* **1991**, *403*, 15. (f) Biradha, K.; Hansen, V. M.; Leong, W. K.; Pomeroy, R. K.; Zaworotko, M. J. *J. Cluster Sci.* **2000**, *11*, 285.

Table 2. Selected Bond Distances (Å) and Angles (deg) for the Isomeric Triosmium Clusters 2b and 2c[a]

Cluster **2b**

Bond Distances

Os(1)−Os(2)	2.8642(6)	Os(1)−Os(3)	2.8734(7)
Os(2)−Os(3)	2.8774(6)	P(1)···P(2)	3.863 (4)
Os(1)−P(1)	2.307(2)	Os(2)−P(2)	2.314(2)
C(1)−C(2)	1.32(1)		

Bond Angles

P(1)−Os(1)−Os(2)	159.83(5)	P(1)−Os(1)−Os(3)	101.88(6)
P(2)−Os(3)−Os(1)	100.27(6)	P(2)−Os(3)−Os(2)	157.10(5)
C(27)−Os(1)−Os(2)	93.8(3)	C(27)−Os(1)−Os(3)	80.4(3)
C(36)−Os(1)−Os(2)	83.0(2)	C(36)−Os(1)−Os(3)	94.1(3)
C(29)−Os(2)−Os(1)	82.3(3)	C(29)−Os(2)−Os(3)	93.7(3)
C(32)−Os(2)−Os(1)	95.3(3)	C(32)−Os(2)−Os(3)	77.7(3)
C(34)−Os(3)−Os(1)	78.6(3)	C(34)−Os(3)−Os(2)	97.6(2)
C(35)−Os(3)−Os(1)	97.0(3)	C(35)−Os(3)−Os(2)	81.9(3)
C(1)−P(1)−Os(1)	122.1(3)	C(2)−P(2)−Os(3)	121.4(3)
C(2)−C(1)−P(1)	134.2(6)	C(1)−C(2)−P(2)	134.0(6)

Cluster **2c**

Bond Distances

Os(1)−Os(2)	2.9218(5)	Os(1)−Os(3)	2.9286(5)
Os(2)−Os(3)	2.8914(5)	P(1)···P(2)	3.092 (6)
Os(1)−P(1)	2.293(2)	Os(1)−P(2)	2.299(2)
C(1)−C(2)	1.322(9)		

Bond Angles

P(1)−Os(1)−P(2)	84.66(7)	P(1)−Os(1)−Os(2)	167.54(5)
P(2)−Os(1)−Os(2)	107.62(5)	P(1)−Os(1)−Os(3)	108.61(5)
P(2)−Os(1)−Os(3)	166.48(5)	C(27)−Os(1)−Os(2)	92.9(2)
C(27)−Os(1)−Os(3)	85.2(2)	C(28)−Os(1)−Os(2)	86.4(2)
C(28)−Os(1)−Os(3)	92.4(2)	C(29)−Os(2)−Os(3)	91.7(2)
C(29)−Os(2)−Os(1)	86.5(2)	C(32)−Os(2)−Os(3)	84.9(2)
C(32)−Os(2)−Os(1)	90.7(2)	C(34)−Os(3)−Os(2)	92.2(2)
C(34)−Os(3)−Os(1)	84.8(2)	C(36)−Os(3)−Os(2)	85.3(2)
C(36)−Os(3)−Os(1)	91.6(2)	C(1)−P(1)−Os(1)	109.0(3)
C(2)−P(2)−Os(1)	107.8(3)	C(2)−C(1)−P(1)	118.1(6)
C(1)−C(2)−P(2)	120.2(6)		

[a] Numbers in parentheses are estimated standard deviations in the least significant digits.

P-substituted Os$_3$ and Ru$_3$ clusters,[29] as supported by molecular mechanics calculations.[30] The P(1)−Os(1) (2.307(2) Å) and P(2)−Os(3) (2.314(2) Å) distances are in excellent agreement with the average lengths reported for a variety of P-substituted osmium compounds.[31] Coordination of the diphosphine ligand across the Os(1)−Os(3) bond in **2b** results in a significant stretching of the (*Z*)-Ph$_2$PCH=CHPPh$_2$ ligand, which leads to ground-state destabilization relative to the chelating isomer **2c**. The internuclear P(1)···P(2) distance of 3.863(4) Å found for **2b** is ca. 0.58 Å longer than the corresponding distance reported for the free ligand (*Z*)-Ph$_2$PCH=CHPPh$_2$, while the P(1)−C(1)−C(2) and P(2)−C(2)−C(1) bond angles of 134.2(6) and 134.0(6)°, respectively, associated with the unsaturated backbone of the diphosphine ligand are ca. 11° larger as compared to the analogous linkages in (*Z*)-Ph$_2$PCH=CHPPh$_2$.[32] Additional evidence supporting the unfavorable bridging mode of coordination of the unsaturated phosphine to the metal frame in **2b** is seen in the C(1)−P(1)−Os(1) (122.1(3)°) and C(2)−P(2)−Os(2) (121.7(3)°) bond angles, which exhibit a substantial deviation from the anticipated bond angle of ca. 109° expected for a tetracoordinate phosphorus center.

The molecular structure of **2c** shown in Figure 1 confirms the attendant migration of the diphosphine ligand upon heating cluster **2b**. The mean Os−Os and Os−P bond lengths were computed as 2.9139 and 2.296 Å, respectively, and are unremarkable with respect to **2b** and other phosphine-substituted osmium clusters. The 10 ancillary carbonyls are all linear in nature and reveal a slight twist or canting of the axial CO groups, albeit much less pronounced than the twist observed in **2b**. The nonbonding P(1)···P(2) bond distance of 3.092(6) Å in **2c** is nearly 0.77 Å shorter than the internuclear P(1)···P(2) separation in **2b** and is in keeping with the trend reported for the free ligand (vide supra) and other mono- and polynuclear compounds containing a chelating (*Z*)-Ph$_2$PCH=CHPPh$_2$ ligand.[10,11,33] Consistent with our premise concerning the greater stability for chelation of the (*Z*)-Ph$_2$PCH=CHPPh$_2$ ligand in **2c** vis-á-vis cluster **2b** are the angles of 109.0(3), 107.8(3), 120.2(6), and 118.1(6)° found for the Os(1)−P(1)−C(1), Os(1)−P(2)−C(2), P(1)−C(1)−C(2), and P(2)−C(2)−C(1) linkages, respectively. These values show minimal deviation from the idealized bond angles of 109° for phosphorus and 120° for carbon.

III. Kinetic Data for Diphosphine Ligand Isomerization in Os$_3$(CO)$_{10}$[(*Z*)-Ph$_2$PCH=CHPPh$_2$]. The isomerization reaction involving **2b** and **2c** was investigated by both UV−vis and ^{31}P NMR spectroscopy, with the latter analytical method providing unequivocal evidence for the reversible equilibrium between **2b** and **2c**. The approach to equilibrium for the conversion of **2b** to **2c** was monitored by ^{31}P NMR spectroscopy in toluene-d_8 at 358.0 and 373.0 K, with the data from the latter temperature displayed in Figure 2. The plot of the total Os$_3$ concentration versus time reveals smooth exponential decay and growth curves for the consumption and formation of clusters **2b**,**c**, respectively. Nonlinear regression analysis of these data afforded a first-order rate constant for the consumption of **2b** (k_e = [1.82(4)] × 10^{-4} s^{-1}) that was nearly identical with the rate determined for the formation of **2c** (k_e = [1.74(2)] × 10^{-4} s^{-1}). The rate constants (k_e) reported for the two ^{31}P NMR experiments in Table 3 represent an average of the reaction rates from the decay and growth curves of cluster **2**. The final ^{31}P NMR spectrum in Figure 2 recorded after 11 h of thermolysis (>10 half-lives) clearly favors the chelating isomer (δ 37.86) and affords K_{eq} = 6.9 (at 373 K) for the **2b** ⇄ **2c** isomerization. An identical K_{eq} value was determined from the ^{31}P NMR experiment conducted at 358.0 K.[34] With the K_{eq} value in hand, the first-order rate constants k_1 and k_{-1}, as defined in Scheme 1, are readily extracted and are

---

[29] (a) Alex, R. F.; Einstein, F. W. B.; Jones, R. H.; Pomeroy, R. K. *Inorg. Chem.* **1987**, *26*, 3175. (b) Bruce, M. I.; Liddell, M. J.; Hughes, C. A.; Skelton, B. H.; White, A. H. *J. Organomet. Chem.* **1988**, *347*, 157. (c) Bruce, M. I.; Liddell, M. J.; Hughes, C. A.; Patrick, J. M.; Skelton, B. H.; White, A. H. *J. Organomet. Chem.* **1988**, *347*, 181. (d) Bruce, M. I.; Liddell, M. J.; Skawkataly, O. B.; Hughes, C. A.; Skelton, B. H.; White, A. H. *J. Organomet. Chem.* **1988**, *347*, 207.

[30] Lauher, J. W. *J. Am. Chem. Soc.* **1986**, *108*, 1521.

[31] Orpen, A. G.; Brammer, L.; Allen, F. K.; Kennard, O.; Watson, D. G.; Taylor, R. *J. Chem. Soc., Dalton Trans.* **1989**, S1.

[32] Berners, S. J.; Colquhoun, L. A.; Healy, P. C.; Byriel, K. A.; Hanna, J. V. *J. Chem. Soc., Dalton Trans.* **1992**, 3357.

[33] (a) Yang, K.; Bott, S. G.; Richmond, M. G. *Organometallics* **1994**, *13*, 3788. (b) Watson, W. H.; Ejsmont, K.; Liu, J.; Richmond, M. G. *J. Chem. Crystallogr.* **2003**, *33*, 775.

[34] The equilibrium constant for the **2b** ⇄ **2c** isomerization at each of the temperatures reported in Table 3 was also determined by ^{31}P NMR spectroscopy. The calculated K_{eq} values were found to be relatively temperature insensitive and yielded an average value of 6.9, which was employed in extraction of the individual rate constants associated with the isomerization reaction.

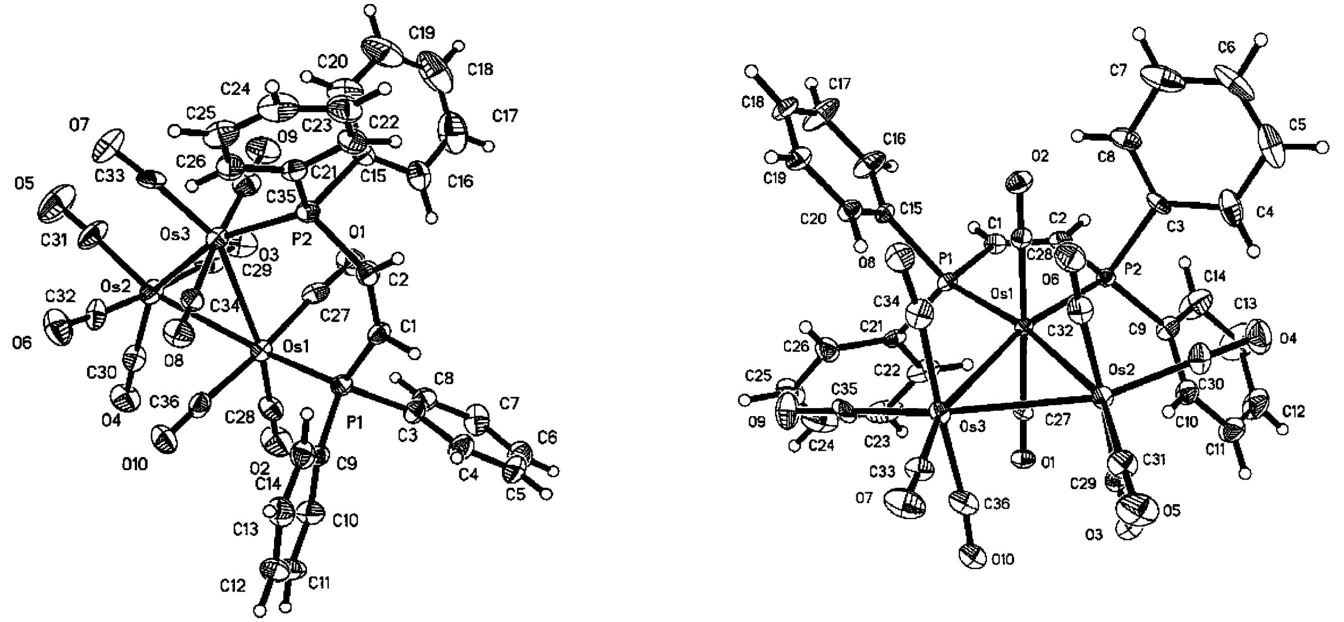

Figure 1. Thermal ellipsoid plots of the bridging (left) and chelating (right) isomers of $Os_3(CO)_{10}[(Z)\text{-}Ph_2PCH{=}CHPPh_2]$, showing the thermal ellipsoids at the 50% probability level.

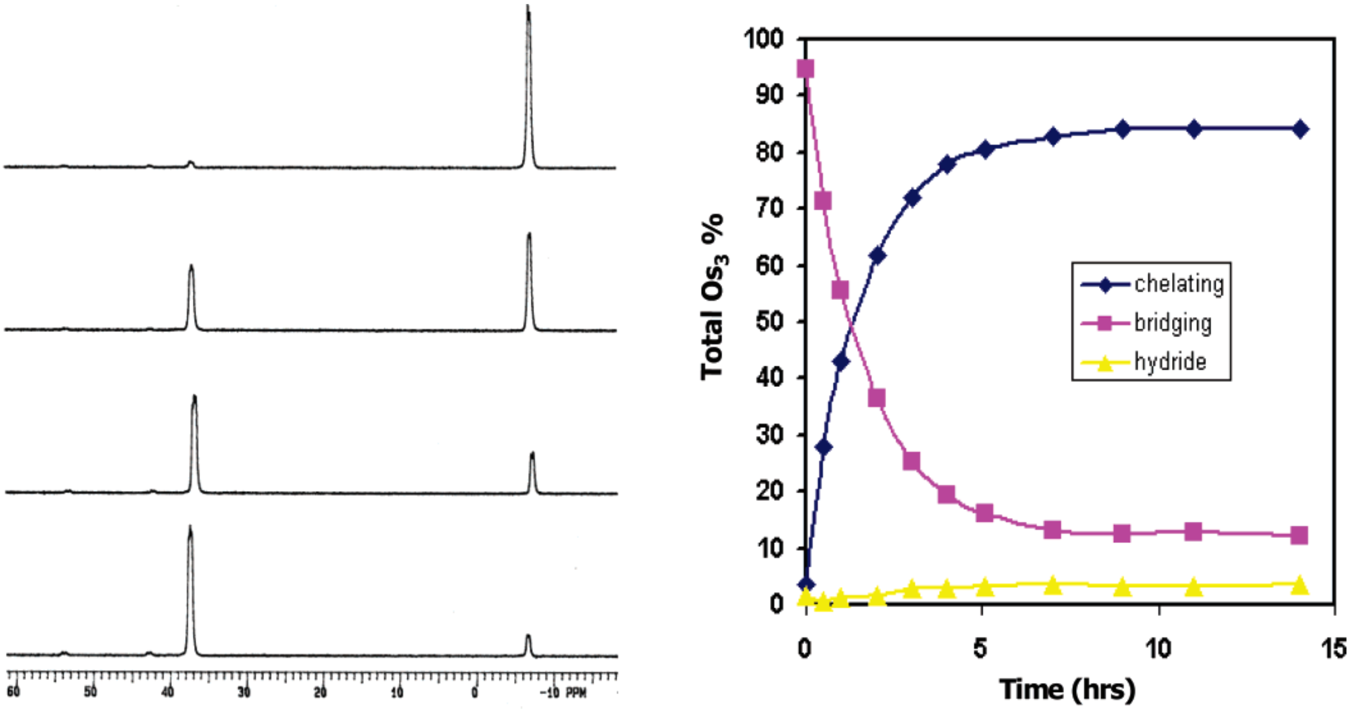

Figure 2. Representative ^{31}P NMR spectra (left) recorded at 373 K in toluene-d_8 for **2b** $\rightleftarrows$ **2c** and the resulting plot for the disappearance of **2b** and the appearance of **2c** and $HOs_3(CO)_9[\mu\text{-}(Z)\text{-}PhP(C_6H_4)CH{=}CHPPh_2]$ (right). The bottom ^{31}P NMR spectrum was recorded after 11 h of thermolysis.

reported in Table 3.[35] Finally, the hydride cluster observed in Figure 2 at δ 43 and 54 after 11 h of thermolysis accounted for less than 4% of the total Os_3 concentration.

The kinetics for the isomerization reaction were also studied by UV−vis spectroscopy in toluene solution under 1 atm of CO over the temperature range of 358.5−381.5 K by following the increase in the absorbance of the 368 nm band belonging to **2c**. The UV−vis spectral changes for the thermolysis of **2b** in toluene carried out at 373 K are shown in Figure 3, where clearly defined isosbestic points at 394 and 437 nm are seen to accompany the reaction. The excellent fit between the least-squares regression curve and the absorbance data (Figure 3) confirms that the isomerization is well-behaved and free from complications. Unlike the ^{31}P NMR experiments, where the thermally promoted loss of CO in **2c** gives rise to small quantities of the hydride cluster $HOs_3(CO)_9[\mu\text{-}(Z)\text{-}PhP(C_6H_4)CH{=}$

---

(35) (a) The values for k_1 and k_{-1} for a reversible first-order process were computed with the aid of the following equations: $k_1 = k_e/[1 + K_{eq}^{-1}]$ and $k_{-1} = k_e/[1 + K_{eq}]$. (b) For a detailed derivation of the integrated rate expression of a reversible first-order reaction, see: Espenson, J. H. *Chemical Kinetics and Reaction Mechanisms*, 2nd ed.; McGraw-Hill: New York, 1995.

Table 3. Kinetic Data for the Isomerization of 2b and 2c in Toluene[a]

temp (K)	$10^4 k_e$ (s^{-1})[b]	$10^4 k_1$ (s^{-1})	$10^4 k_{-1}$ (s^{-1})	method
358.0	0.37 ± 0.01	0.32 ± 0.01	0.05 ± 0.01	^{31}P NMR
358.5	0.40 ± 0.01	0.35 ± 0.01	0.05 ± 0.01	UV−vis
364.0	0.66 ± 0.01	0.58 ± 0.01	0.08 ± 0.01	UV−vis
369.0	1.16 ± 0.02	1.01 ± 0.02	0.15 ± 0.02	UV−vis
373.0	1.78 ± 0.04	1.56 ± 0.04	0.22 ± 0.04	^{31}P NMR
373.0	1.76 ± 0.01	1.54 ± 0.01	0.22 ± 0.01	UV−vis
373.0	1.75 ± 0.02			UV−vis[c]
378.0	2.92 ± 0.14	2.55 ± 0.14	0.37 ± 0.14	UV−vis
381.5	3.82 ± 0.12	3.34 ± 0.12	0.48 ± 0.12	UV−vis

[a] All kinetic data were collected under 1 atm of CO unless otherwise noted. The quoted UV−vis kinetic data represent an average of two independent measurements. [b] The quoted rate constants (k_e) represent the rate toward equilibrium, as determined by following the increase in the 368 nm band (UV−vis) and the changes in the ^{31}P resonances for the bridging and chelating isomers (^{31}P NMR). [c] Experiment conducted in a Fischer−Porter tube under 6.8 atm of CO (constant pressure). Only the determined value of k_e is reported here.

CHPPh$_2$], the amount of hydride cluster present in the UV−vis experiments is predicted to be negligible. The equilibrium in Scheme 1 mandates the suppression of the hydride cluster for reactions carried out under high concentrations of CO relative to cluster **2**. A conservative 10-fold concentration excess of CO relative to the bridging and chelating cluster **2** is predicted from available solubility data for CO in toluene.[36] The rate constants for the approach to equilibrium (k_e), along with the values of k_1 and k_{-1}, as computed with the aforementioned K_{eq} value for **2b** $\rightleftarrows$ **2c**, are given in Table 3.[37] The UV−vis data collected at 373 K furnished values for k_e, k_1, and k_{-1} in excellent agreement with those values determined by the ^{31}P NMR experiment, underscoring the validity of the data obtained from the two different experiments. That the presence of added CO does not affect the equilibrium between **2b** and **2c** was demonstrated by the reaction conducted under 6.8 atm of CO. Here the value of $[1.75(2)] \times 10^{-4}$ s^{-1} found for k_e is within experimental error to the corresponding reaction run under 1 atm of CO.

Eyring plots of $\ln(k_1/T)$ and $\ln(k_{-1}/T)$ versus T^{-1} allowed for the determination of the isomerization activation parameters for the forward and reverse reaction directions in cluster **2**. The calculated values of $\Delta G^{\ddagger}_{373} = 28.4(6)$ kcal/mol, $\Delta H^{\ddagger} = 26.5(6)$ kcal/mol, and $\Delta S^{\ddagger} = -5(2)$ eu for the forward isomerization (**2b** → **2c**) and $\Delta G^{\ddagger}_{373} = 29.9(6)$ kcal/mol, $\Delta H^{\ddagger} = 26.5(6)$ kcal/mol, and $\Delta S^{\ddagger} = -9(2)$ eu for the reverse isomerization (**2c** → **2b**) reveal that the entropy of activation is small and negative in both directions and argues against a dissociative mechanism involving the release of one of the PPh$_2$ moieties from the cluster frame to generate an unsaturated Os$_3$ cluster having a pendant η^1-diphosphine moiety. Such a phosphine ligand release process that exhibits a positive $\Delta S^{\ddagger}$ value has been demonstrated by Goldberg in the reductive coupling of ethane from PtMe$_4$(dppe).[38] There the rate-limiting chelate opening of the diphosphine ligand in PtMe$_4$(dppe) furnishes a reactive five-coordinate intermediate that serves as the platform for the evolution of ethane.[39]

IV. Diphosphine Isomerization Mechanism. Any acceptable mechanism for the isomerization of the (*Z*)-Ph$_2$PCH=CHPPh$_2$ ligand about the triosmium frame must account for the observed P ligand/CO exchange that accompanies the reaction. A terminal−bridge−terminal sequence involving a CO group(s) and a PPh$_2$ moiety across an Os−Os bond(s) would effectively serve to scramble the participant ligands. The highly ordered transition state mandated by any such terminal−bridge−terminal sequence is reconciled with the negative $\Delta S^{\ddagger}$ values found from Eyring analysis of the rate data. A rate-limiting process involving the dissociation or release of one of the arms of the bidentate ligand, followed by scrambling of the diphosphine and subsequent ligand ring closure (bridge or chelate), can be immediately eliminated from consideration, as it would violate the observed entropies of activation and insensitivity of the reaction to added CO.

The top portion of Scheme 2 depicts a pairwise terminal−bridge exchange in cluster **2b** involving an axial group (CO$_a$) and one P moiety across the diphosphine-bridged Os−Os bond that proceeds through the doubly bridged cluster Os$_3$(CO)$_9$(μ-CO)[(*Z*)-μ,η^1-Ph$_2$PCH=CHPPh$_2$]. This species can produce the chelating isomer **2c** ultimately upon opening of the μ-CO and μ-phosphine bridges. However, the simple opening of this doubly bridged cluster cannot give **2c** directly, as an additional permutation(s) or turnstile rotation(s) of the remaining spectator groups associated with the phosphine-substituted osmium centers must accompany the bridge-opening reaction. A more direct diphosphine equilibration that relies on the well-known “merry-go-round” mechanism is illustrated in the bottom portion of Scheme 2. Here a terminal−bridge exchange of two equatorial CO groups and one of the phosphine centers in **2b** gives rise to the triply bridged cluster Os$_3$(CO)$_8$(μ-CO)$_2$[(*Z*)-μ,η^1-Ph$_2$PCH=CHPPh$_2$], which directly furnishes **2c** upon completion of the bridge−terminal exchange.[40,41] We favor the latter mechanism for diphosphine isomerization in Os$_3$(CO)$_{10}$[(*Z*)-Ph$_2$PCH=CHPPh$_2$], on the basis of its simplicity.[42] Given that no dynamic diphosphine isomerization has been observed in Os$_3$(CO)$_{10}$(dppe),[1a] the saturated analogue of **2**, we submit that the stereochemistry and rigid nature of the ancil-

---

(36) (a) Van Raaij, E. U.; Schmulbach, C. D.; Brintzinger, H. H. *J. Organomet. Chem.* **1987**, *328*, 275. (b) Basickos, L.; Bunn, A. G.; Wayland, B. B. *Can. J. Chem.* **2001**, *79*, 854.

(37) A caveat worth pointing out is that the reversible first-order behavior for the **2b** $\rightleftarrows$ **2c** equilibrium could have easily been misinterpreted as an irreversible first-order conversion involving **2b** $\rightleftarrows$ **2c** had the UV−vis data been analyzed in the absence of the ^{31}P NMR data.

(38) Crumpton-Bregel, D. M.; Goldberg, K. I. *J. Am. Chem. Soc.* **2003**, *125*, 9442.

(39) For some other examples exhibiting chelate-ring opening, see: (a) Knebel, W. J.; Angelici, R. J. *Inorg. Chem.* **1974**, *13*, 627, 632. (b) Schultz, L. D.; Dobson, G. R. *J. Organomet. Chem.* **1976**, *124*, 19. (c) Dobson, G. L.; Cortés, J. E. *Inorg. Chem.* **1988**, *27*, 3308. (d) Henderson, R. A. *J. Chem. Soc., Dalton Trans.* **1988**, 509, 515.

(40) In principle the VT ^{13}C NMR spectra of both **2b** and **2c** could provide critical data capable of differentiating the two proposed diphosphine scrambling mechanisms. Unfortunately, the complete coalescence of all carbonyl groups in **2b** and **2c** by 363 K does not allow the ^{13}C NMR data to distinguish between the two mechanisms depicted in Scheme 2.

(41) The scrambling of the carbonyl groups in **2b** and **2c** followed terminal−bridge−terminal merry-go-round and turnstile processes found in other phosphine-substituted Os$_3$ clusters. For related VT NMR studies, see: (a) References 1c,d. (b) Deeming, A. J.; Donovan-Mtunzi, S,; Kabir, S. E. *J. Organomet. Chem.* **1985**, *281*, C43. (c) Alex, R. F.; Pomeroy, R. K. *Organometallics* **1987**, *6*, 2437.

(42) The simplicity alluded to stems from the application of Occam’s razor.

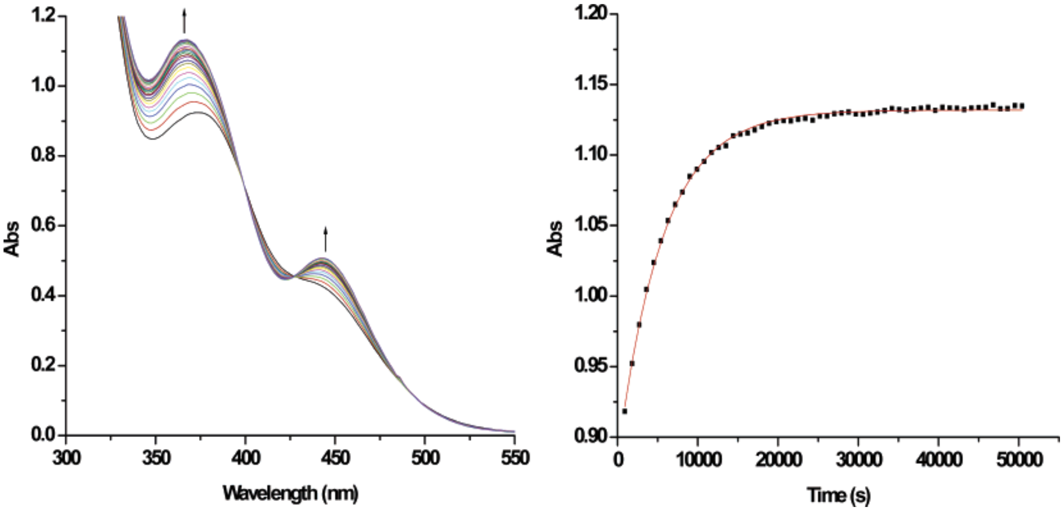

Figure 3. UV-vis spectral changes for **2b** ⇄ **2c** recorded at 373 K in toluene (left) and the absorbance versus time curves for the experimental data (■) and the least-squares fit of k_e (right).

Scheme 2

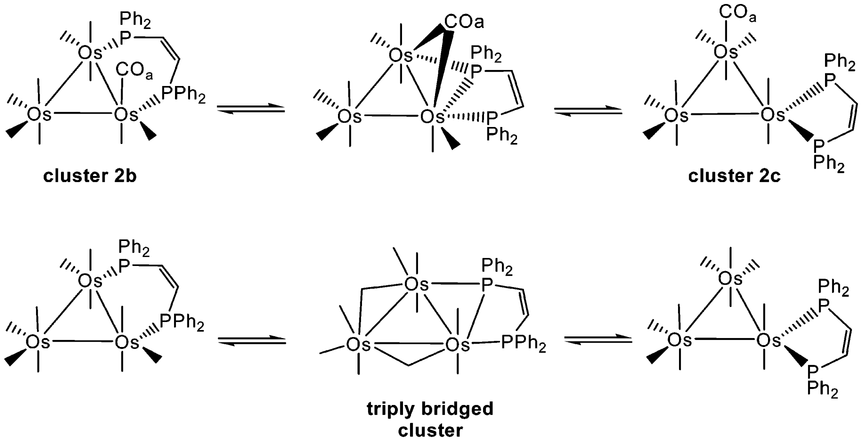

lary (Z)-Ph$_2$PCH=CHPPh$_2$ ligand actually promote the scrambling of the ligand about the cluster by maintaining constant and intimate contact between the diphosphine ligand and the osmium centers.[43] We believe that this isomerization phenomenon is general in nature, at least for this genre of cluster, provided that the diphosphine ligand is rigid and possesses cis stereochemistry, based on our observations of facile diphosphine isomerization in the cluster compounds Os$_3$(CO)$_{10}$(P−P) (where P−P = bpcd, 3,4-bis(diphenylphosphino)-5-methoxy-2(5H)-furanone (bmf), 1,2-bis(diphenylphosphino)benzene).[44,45]

The dynamic migration of CO ligands about the metal centers in polynuclear clusters through terminal ⇄ bridge ⇄ terminal CO exchanges has been a phenomenologically established fact for over 3 decades.[46] Analogous migratory ligand behavior has only recently been observed for tertiary phosphine ligands. For example, Adams has provided conclusive NMR evidence for the intramolecular scrambling of phosphine ligands between the platinum and adjacent ruthenium centers in the mixed-metal carbide clusters PtRu$_5$(μ_6-C)(CO)$_{15}$P,[47] while phosphine equilibration between the two ruthenium centers in the dinuclear compounds Cp*$_2$Ru$_2$(μ-H)$_2$P has been demonstrated by Suzuki.[48,49] The postulated transformation of an η^1-phosphine ligand to a μ-bound phosphine in our work and the above examples is strengthened by reports showing the coordination of a tertiary P ligand simultaneously to two and three metal centers.[50]

---

(43) In the case of an isomerization reaction involving a dppe ligand, we can envision an intermediate state where the hydrogen atoms of the ethane backbone must adopt an eclipsed conformation during the bridge ⇄ chelate transformation. This specific destabilization is avoided in diphosphines possessing an unsaturated carbon backbone.

(44) Unpublished results.

(45) Our isomerization data for **2b** ⇄ **2c** parallel those of Os$_3$(CO)$_{10}$(Ph$_2$PCH$_2$CH$_2$SMe), where thiophosphine isomerization is believed to proceed through a bridging thioether moiety. See: Persson, R.; Monari, M.; Gobetto, R.; Russo, A.; Aime, S.; Calhorda, M. J.; Nordlander, E. *Organometallics* **2001**, *20*, 4150.

(46) (a) Cotton, F. A. *Inorg. Chem.* **1966**, *6*, 1083. (b) Johnson, B. F. G.; Lewis, J.; Reichert, B. E.; Schorpp, K. L. *J. Chem. Soc., Dalton Trans.* **1976**, 1403. (c) Cotton, F. A.; Hanson, B. E. In *Rearrangements in Ground and Excited States*; de Mayo, P., Ed.; Academic Press: New York, 1980; Chapter 12.

(47) Adams, R. D.; Captain, B.; Fu, W.; Pellechia, P. J. *Inorg. Chem.* **2003**, *42*, 3111.

(48) Ohki, Y.; Suzuki, H. *Angew. Chem., Int. Ed.* **2002**, *41*, 2994.

(49) For additional reports of phosphine-ligand isomerization in metal clusters, see: (a) Laurenczy, G.; Bondietti, G.; Ros, R.; Roulet, R. *Inorg. Chim. Acta* **1996**, *247*, 65. (b) Braunstein, P.; Boag, N. M. *Angew. Chem., Int. Ed.* **2001**, *40*, 2427. (c) Bradford, A. M.; Douglas, G.; Manojloviæ-Muir, L.; Muir, K. W.; Puddephatt, R. J. *Organometallics* **1990**, *9*, 409.

(50) (a) Balch, A. L.; Davis, B. J.; Olmstead, M. M. *J. Am. Chem. Soc.* **1990**, *112*, 8592; *Inorg. Chem.* **1993**, *32*, 3937. (b) Pechmann, T.; Brandt, C. D.; Werner, H. *Angew. Chem., Int. Ed.* **2000**, *39*, 3909; *Chem. Commun.* **2003**, 1136. (c) Pechmann, T.; Brandt, C. D.; Roger, C.; Werner, H. *Angew. Chem., Int. Ed.* **2002**, *41*, 2301.

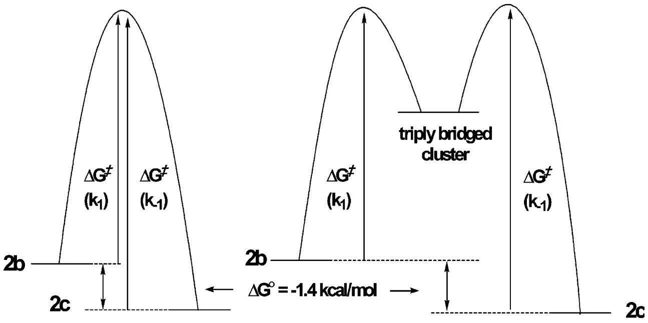

Figure 4. Free-energy diagrams for the merry-go-round isomerization of **2b** ⇄ **2c** at 373 K where the triply bridged cluster $Os_3(CO)_8(\mu\text{-}CO)_2[(Z)\text{-}\mu,\eta^1\text{-}Ph_2PCH{=}CHPPh_2]$ functions as a transition state (left) and as a discrete intermediate of finite lifetime (right).

Finally, Figure 4 shows two free-energy diagrams for the merry-go-round isomerization for **2b** ⇄ **2c** at 373 K, whose major difference lies in the nature of the contribution of the putative species $Os_3(CO)_8(\mu\text{-}CO)_2[(Z)\text{-}\mu,\eta^1\text{-}Ph_2PCH{=}CHPPh_2]$. The left-hand diagram depicts a single-step isomerization where the triply bridged cluster $Os_3(CO)_8(\mu\text{-}CO)_2[(Z)\text{-}\mu,\eta^1\text{-}Ph_2PCH{=}CHPPh_2]$ functions as the transition state for the two isomers of $Os_3(CO)_{10}[(Z)\text{-}Ph_2PCH{=}CHPPh_2]$, while the two-step mechanism involving $Os_3(CO)_8(\mu\text{-}CO)_2[(Z)\text{-}\mu,\eta^1\text{-}Ph_2PCH{=}CHPPh_2]$ as a reactive intermediate of finite lifetime in the **2b** ⇄ **2c** isomerization is shown to the right. Differentiation between the concerted (left) and two-step (right) processes is not a trivial matter, but we would suggest that our data favor the concerted scrambling of the diphosphine ligand. The $\Delta G°$ value of -1.4 kcal/mol in favor of cluster **2c**, as determined from the magnitude of K_{eq} for **2b** ⇄ **2c** by ^{31}P NMR spectroscopy (vide supra), is identical with the $\Delta\Delta G^{\ddagger}$ value found from the kinetic experiments. This is reasonable and expected for a single-step or concerted reaction, with the triply bridged cluster serving as the transition state for both **2b** and **2c**. Theoretical calculations on the bridge-to-chelate isomerization of the $H_2PCH_2CH_2PH_2$ ligand in the dinuclear compound $Mo_2Cl_4(H_2PCH_2CH_2PH_2)_2$ reveal that a nondissociative migration of the phosphine moieties across the Mo−Mo quadruple bond, analogous to that proposed by us in $Os_3(CO)_8(\mu\text{-}CO)_2[(Z)\text{-}\mu,\eta^1\text{-}Ph_2PCH{=}CHPPh_2]$, proceeds as a transition state and not a bona fide intermediate.[51,52] If the two-step process reflects the scrambling mechanism, then the fortuitous similarity in the values determined for $\Delta G°$ and $\Delta\Delta G^{\ddagger}$ indicate that the barrier heights relating **2b** and **2c** to the triply bridged cluster $Os_3(CO)_8(\mu\text{-}CO)_2[(Z)\text{-}\mu,\eta^1\text{-}Ph_2PCH{=}CHPPh_2]$ must be small and identical in magnitude.

Conclusions

The reaction between $Os_3(CO)_{10}(MeCN)_2$ and $(Z)\text{-}Ph_2PCH{=}CHPPh_2$ gives $1,2\text{-}Os_3(CO)_{10}[(Z)\text{-}Ph_2PCH{=}CHPPh_2]$ as the kinetic product of ligand substitution. Isomerization of the bridged cluster into the chelated cluster $1,1\text{-}Os_3(CO)_{10}[(Z)\text{-}Ph_2PCH{=}CHPPh_2]$ proceeds readily upon heating. The isomerization kinetics and thermodynamics have been explored by spectroscopic methods and both products subjected to structural analysis. On the basis of the kinetic data, a nondissociative phosphine migration across one of the Os−Os bonds has been proposed. The generality of this type of ligand isomerization as a function of metal cluster and diphosphine ligand will be probed by our groups, with our data reported in due course.

Acknowledgment. We thank Professor Jim Espenson for his advice concerning the nonlinear regression treatment of our UV−vis data and Professor Paul Marshall for his shared insights during our infrequent luncheons. Financial support from the Robert A. Welch Foundation (Grant No. P-074, W.H.W.; Grant No. B-1093, M.G.R.) is greatly appreciated.

Supporting Information Available: Tables giving crystallographic data for the bridging and chelating isomers of $Os_3(CO)_{10}[(Z)\text{-}Ph_2PCH{=}CHPPh_2]$. This material is available free of charge via the Internet at http://pubs.acs.org. Crystallographic data for the structural analyses have also been deposited with the Cambridge Crystallographic Data Center: CCDC No. 274229 for $1,2\text{-}Os_3(CO)_{10}[(Z)\text{-}Ph_2PCH{=}CHPPh_2]\cdot CH_2Cl_2$ and CCDC No. 274230 for $1,1\text{-}Os_3(CO)_{10}[(Z)\text{-}Ph_2PCH{=}CHPPh_2]$. Copies of this information may be obtained free of charge from the Director, CCDC, 12 Union Road, Cambridge CB2 1EZ, U.K. (fax, +44(1223)336−033; e-mail, deposit@ccdc.ac.uk; web, http://www:ccdc.cam.ac.uk).

OM0505413

---

(51) Blasco, S.; Demachy, I.; Jean, Y.; Lledos, A. *New J. Chem.* **2002**, *26*, 1118.

(52) In a subsequent paper by the same researchers, it was disclosed that a multistep process involving the dissociative release of one arm of the diphosphine ligand, followed by phosphine migration and ligand reattachment, was energetically competitive with the concerted phosphine migration process reported in ref 51. Since a dissociative mechanism is not supported by our kinetic data, we can exclude it from consideration. See: Demachy, I.; Jean, Y.; Lledos, A. *New J. Chem.* **2004**, *28*, 1494.